INTERNATIONAL JOURNAL OF INNOVATIVE RESEARCH & DEVELOPMENT

ISSN 2278 – 0211 (Online)

Structural Study of (1-x) $(Bi_{0.5}Na_{0.5})$ TiO_3 -x$LiNbO_3$ Solid-Ceramics

Varsha Sao
Research Scholar, Dr. C. V. Raman University, Kota, Bilaspur, Chhattisgarh, India

Abstract:
Bismuth sodium titante Lithium Niobate (1-x)$(Bi_{0.5}Na_{0.5})TiO_3$-x$LiNbO_3$ where (x=0.01,0.02,0.03)[BNTLN] which is a lead free antimony are prepared by conventional method of solid state reaction method. BNTLN samples are selected such that density about 95% of theoretical values. The phase formation was confirmed by X-ray diffraction (XRD). $Bi_{0.5}Na_{0.5}TiO_3$ was investigated by XRD and Raman spectroscopy for phase formation and local structure. The density and grain size depend upon Li,Nb concentration and found propsanal to $LiNbO_3$ concentration. In X-ray diffraction patterns the peak decreases with increase in $LiNbO_3$. In Preliminary crystal-structure analysis shows the existence of phase transition from rhombhedral to a hexagonal structure.
A splitting of (TO3) mode at x=0.03. With increase in x change in peak position, width and intensity respectively has been noticed in Raman spectrum with increase in $LiNbO_3$ concentration piezoelectric properties increase and found optimum at x=0.03.This optimum value is due to co-existence of two ferroelectric phases. Thus it is conducted that morphotropic phase boundary in (1-x)$(Bi_{0.5}Na_{0.5})TiO_3$-x$LiNbO_3$ lies for composition x=0.03.

Keywords: *Ceramics, X-ray diffraction, Raman spectroscopy*

1. Introduction

Lead-based complex perovskite relaxor ferroelectrics, such as $Pb(Mg_{1/3}Nb_{2/3})O_3$ (PMN), $Pb(Zn_{1/3}Nb_{2/3})O_3$, and the derived compounds, are widely used in the fabrication of multilayer ceramics capacitors, hysteresis-free actuators, and high performance sensors because of their excellent dielectric and piezoelectric properties.[1–4] However, these lead based relaxor ferroelectrics contain more than 60 wt % lead.[5,6] Lead is a very toxic substance, which can cause damage to the kidney, brain, and nervous system, especially the intelligence of the children.[7] In recent years, therefore, some countries have required all new electronic products to be lead-free for the environmental protection and human health.[8]

Pure BNT is an A-site complex perovskite-structured ferroelectric with rhombohedral symmetry at room temperature. It has a high Curie temperature (*Tc* = 320 °C) with strong ferroelectricity (*Pr* = 38 μC/cm2) [9–11]. However, the major drawback with BNT is the poling treatment because of its high coercive field (*Ec* = 7.3 kV/mm), resulting in relatively weak piezoelectric properties (*d33* = 70–80 pC/N). Decreasing coercive field and improving the poling process formation of BNT-based solid solution with a morphotropic phase boundary (MPB) is an effective way as proposed and studied by many researchers. Recently many binary or ternary BNT-based MPBs have been reported in literature [12-13].MPBs Are dependent only on composition and are independent of temperature, meaning that compositions near these boundaries should experience little change in the piezoelectric response over a wide temperature range.

$Bi_{0.5}Na_{0.5}TiO_3$ (BNT) is one of the most investigated classical ferroelectric materials having high dielectric constant, piezoelectric coefficient, electrooptic coefficients, broad wavelength sensitivity range, high crystalline uniformity, and it displays a large variety of nonlinear optical effects. It was anticipated that the structure of the solid-solution with a low BT content would become tetragonal due to the rather large lattice distortion of BT compared to the rhombohedral distortion in BNT. Although this structural modification was conformed in earlier works, exclusive studies regarding MPB are rare in the literature [14-18]. Rietveld refinements, Raman spectroscopy and piezoelectric studies have been used as effective techniques to investigate the structural evolution in perovskite solid-solutions. Only, limited reports are available on Raman spectroscopy studies but Rietveld refinements are not well reported in BNT-based systems [18-24]. The present manuscript reports the detailed structural study (X-ray diffraction, Rietveld refinement, Raman spectroscopy) and piezoelectric behaviour by electromechanical factors.

2. Methods

Niobate (1-x)($Bi_{0.5}Na_{0.5}$)TiO_3-x$LiNbO_3$ compositions were prepared using the mixed-oxide method incorporating Bi_2O_3,Na_2CO_3,TiO_2 and Li_2CO_3,Nb_2O_5 (> 99%) in stoichiometric proportions. The mixed powders were ball calcined (1-x)($Bi_{0.5}Na_{0.5}$)-x$LiNbO_3$ milled in ethanol for 24 h using zirconia milling media and calcined at 800°C for 2 h. The powders were then ball milled again for 6 h and uniaxially pressed at a pressure of 5 MPa with a few drops of 3 wt.% polyvinyl alcohol to bind it into disks of 10-mm diameter and 1- to 2-mm thickness.The disks were the sintered at 900°C for 2 h, except for the sample with 0.20 mole fraction $LiNbO_3$ which was sintered at 950°C for 2 h, in air. The X-ray diffractometer (Philip Model X-pert, PANalytical B.V., Almelo, The Netherlands) with CuKa radiation was used to investigate the phase and crystal structure of the sintered ceramics. The preliminary crystal structure details were calculated using the Powder Cell program [32], which is based on the X-ray diffraction pattern of lead-free bismuth (1-x)($Bi_{0.5}Na_{0.5}$)-x$LiNbO_3$ where x = 0.01, 0.02, 0.03 mole fraction) [BNTLN] ceramics. The bulk densities of the sintered ceramics were measured using Archimedes' method. The theoretical density was approximated from the unit cell size and its constituent ions and Raman spectroscopy (Enwave Optronics-Ezraman). The prepared ceramic samples were polarized at room temperature under 35 kV/cm in silicone oil for 20 min.

3. Results and Discussion

Figure 1 a shows the XRD patterns of (1-x)($Bi_{0.5}Na_{0.5}$)-x$LiNbO_3$ ceramics with $0 \leq x \leq 0.03$ sintered at 1150 °C for 4 h. All the compositions exhibit a pure perovskite structure and no second phases are observed, which implies that $LNbO_3$ ceramic has diffused into the $Bi_{0.5}Na_{0.5}TiO_3$ lattices to form a solid-solution. Also Fig. 1b shows the XRD patterns of the ceramics in the 2θ range of 44–50 degree. A distinct 002/200 peak splitting appears when x = 0.03, refer- ring to a hexagonal symmetry. To characterize the phase compositions in a more quantitative way, the XRD patterns of the MPB compositions in the 2θ ranges of 46–48 ° were fitted as shown in Fig. 2. The data show the Lorentzian deconvolution of the 002 and 200 peaks of the tetragonal phase and the 202 peak of the rhombohedral phase. These results suggest that the rhombohedral-hexagonal morphotrophic phase boundary (MPB) of (1-x)($Bi_{0.5}Na_{0.5}$)-x$LiNbO_3$ ceramic is near x = 0.03.

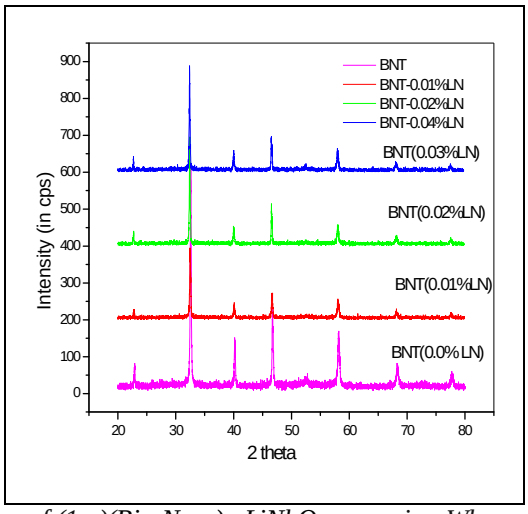

Figure 1(a): X-ray diffraction patterns of (1-x)($Bi_{0.5}Na_{0.5}$)-x$LiNbO_3$ ceramics. Where x = 0.01, 0.02 and 0.03 mole fraction

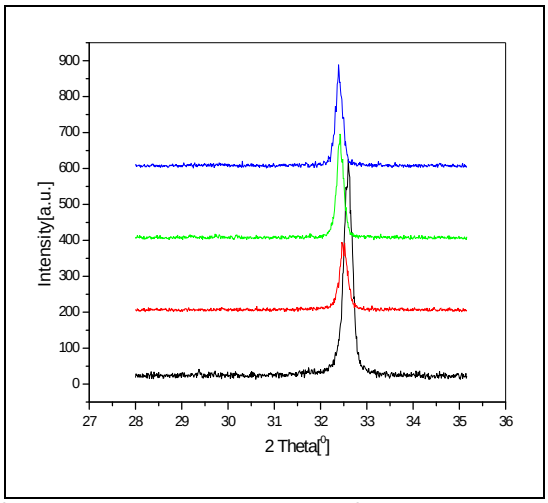

Figure 2(b): X-ray diffraction patterns of of (1-x)($Bi_{0.5}Na_{0.5}$)-x$LiNbO_3$ ceramics for degree 28 to 38. Where x = 0.01,0.02 and 0.03 mole fraction

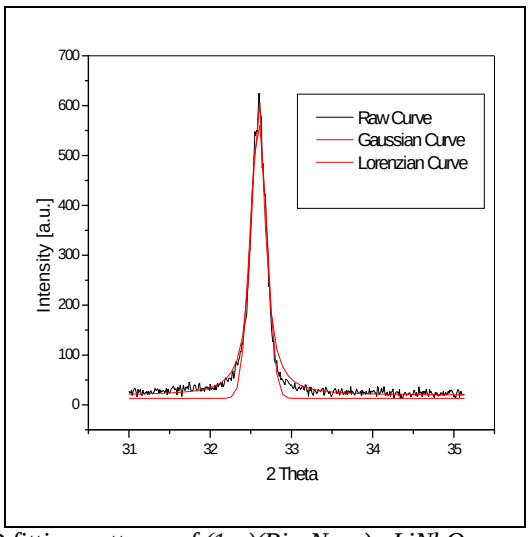

Figure 2(a): XRD fitting patterns of (1-x)($Bi_{0.5}Na_{0.5}$)-x$LiNbO_3$ ceramics with x=0.0

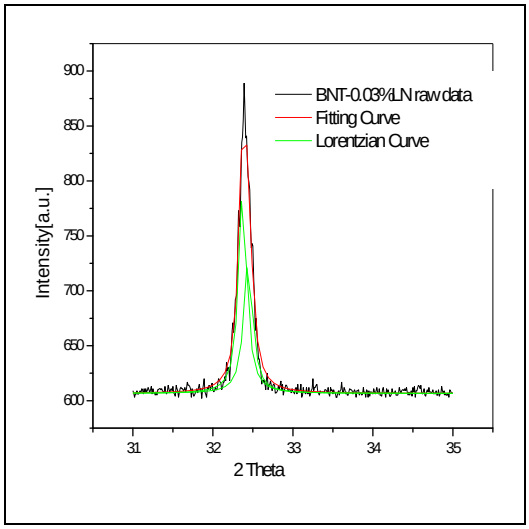

Figure 2(b): XRD fitting patterns of (1-x)($Bi_{0.5}Na_{0.5}$)-x$LiNbO_3$ ceramic with x=0.03

3.1. Raman Spectroscopy Analysis

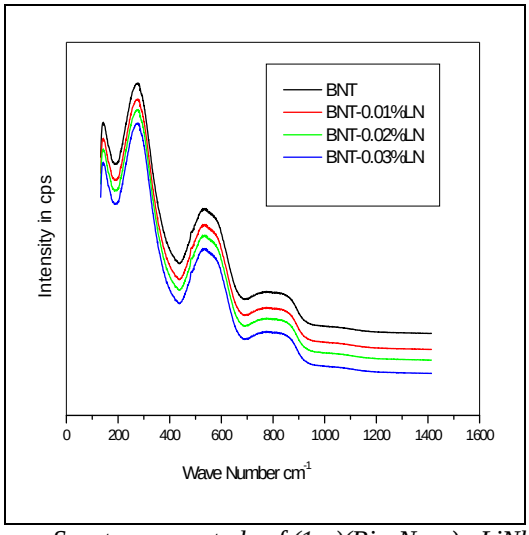

Figure 3: Raman Spectroscopy study of (1-x)($Bi_{0.5}Na_{0.5}$)-x$LiNbO_3$ ceramics

Figure 3 represents the Raman spectroscopy study of (1-x)($Bi_{0.5}Na_{0.5}$)-x$LiNbO_3$ solid solution (x = 0.0–0.03). There are only five Raman-active modes observed in the range from 200 to 14z00 cm−1 in agreement with the works reported by the Rout *et al*. [25] and Eerd *et al*. [26]. BNT ceramics with rhombohedral structure presents 13 Raman-active modes ($\Gamma Raman$ = 4A1 + 9E) due to the disorder in A-site related to distorted octahedral [BiO6] and [NaO6] clusters [27]. The first Raman active A1 (TO1) mode at around (130 cm−1) is related to network modifiers or distorted octahedral [BiO_6] and [NaO_6] clusters. The second Raman active E (TO2) mode can be deconvoluted in three Raman peaks in the regions of 260 cm−1. This mode is assigned to stretching arising from the bonds due to presence of octahedral [TiO6] clusters at short-range. The third Raman-active (LO2) mode with low intensity is related to short-range electrostatic forces associated with the lattice iconicity [28]. According to Dobal *et al*. [36], the (TO3) mode situated at around 625 cm−1 is ascribed to the (O–Ti–O) stretching symmetric vibrations of the octahedral [TiO6] clusters. The (LO3) mode found at 813 cm−1 is due to the presence of the sites within the rhombohedral lattice pre containing octahedral distorted [TiO_6] clusters. These modes are classified into longitudinal (LO) and transverse (TO) components because of the electronic structure with polar character of lattice. There is no significant change in the spectra for the compositions of lower x values (< 0.03). However, the further addition of (x = 0.03) in the solid solution results in anomaly by splitting bands that shift apart from each other.For better observation of the Raman spectra of BNT and BNT-LN (x = 0.05) along with the curves fitted to individual peaks are shown in Fig. 6. The spectra of BNT-$LiNbO_3$ (x = 0.03) show additional peaks around 168,245, 585 and 851 cm−1 compared to the peaks observed in BNT. The occurrence of these new bands, observed band splitting, indicates a structural change at x > 0.03, which are well in line with the studies of XRD phase analysis. All bands appearing in the spectra at x > 0.06 can be assigned to the Raman modes for a tetragonal symmetry [29]. However, from Fig. 3 it is possible to detect that all the Raman peaks are very broad in BNT and BNTLN ceramics. It is believed that this behaviour is due to the presence of the disorder structural or distorted octahedral [TiO6] clusters at short-range and the overlapping of Raman modes due to the lattice anharmonicity. For closer investigation, the variation of full width of half maximum (FWHM) and intensity of individual peaks are plotted in Fig. 6. The mode intensity and FWHM undergo slope change at x = 0.03.

The FWHM of a Raman band is inversely proportional to the lifetime of the corresponding phonon [38],which is in turn closely related to the size of the local (Bi0.5Na0.5)2+TiO3 clusters. When Li^{2+} substitutes for both Bi and Na, Nb^{2+} TiO_3 clusters are formed. As a result, $(Bi_{0.5}Na_{0.5})_2$+TiO_3 clusters are reduced in sizes,giving rise to the peak broadening and intensity weakening of the 280 cm−1 band. There is no change in the frequency of this band since both composition and structure remain the same in the $(Bi_{0.5}Na_{0.5})_2$+TiO_3 clusters when x values are low. With the increase in x value such constraining effect becomes less significant and the phase transition occurs. The variation of intensity and FWHM of all peaks shows a similar type of anomaly at x = 0.03. On the basis of these considerations, it is possible to conclude that the rhombohedral-tetragonal phase co-exists at x = 0.03 which is also observed in the XRD results.

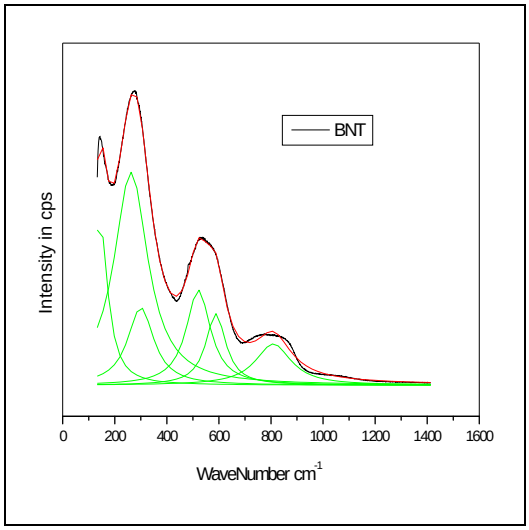

Figure 4(a): Raman Spectra of BNT Black line is the experimental data and green lines are the fitting curve versus $LiNbO_3$ concentration

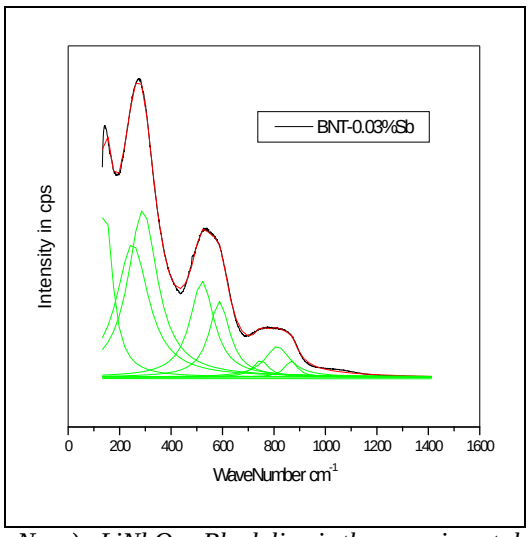

Figure 4(b): Raman Spectra of (1-x) ($Bi_{0.5}Na_{0.5}$)-x$LiNbO_3$ Black line is the experimental data and green lines are the fitting curve versus $LiNbO_3$ concentration

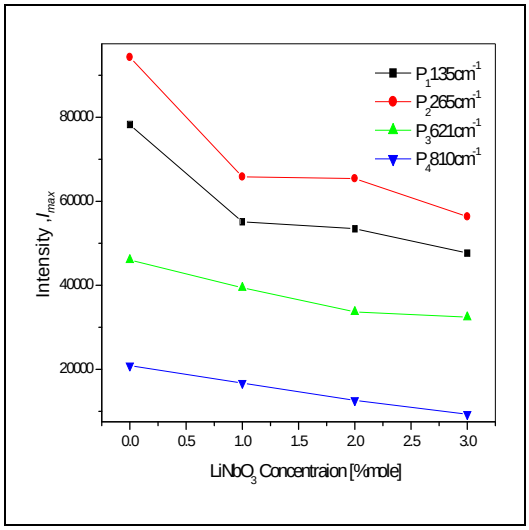

Figure 5: Variation of the intensity of different modes in the Raman spectra versus $LiNbO_3$ Concentration

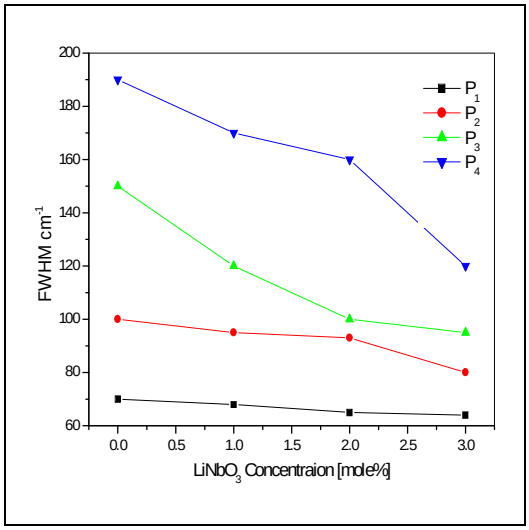

Figure 6: Variation of the FWHM of different modes in the Raman spectra versus $LiNbO_3$ Concentration

4. Conclusion

The solid-solutions $(1-x)(Bi_{0.5}Na_{0.5})-xLiNbO_3$ were successfully synthesized by a conventional solid state reaction rout. X-ray diffraction and Rietveld refinement analysis showed that a morphotropic phase boundary (MPB) exists around $x = 0.03$. Analysis of peak positions, widths and intensities of Raman spectroscopy study also confirmed the existence of morphotropic phase boundary around $x = 0.03$ composition.

5. References

1. L. E. Cross, Ferroelectrics., 76 (1987) 241-67 and reference therein
2. L. E. Cross, Ferroelectrics., 151 (1994) 305-20 and reference therein
3. Z-G Ye, Key Engineering Materials., 155-156(1998) 81-122,
4. Chen, I. W., J. Phys. Chem. Solids., 61(2000) 197-208
5. L. E. Cross, Nature (London), 432(2004) 24-25
6. M. Kosec, V. Bobnar, M. Hrovat, J. Bernard, B. Malic, and J. Holc, J. Mater. Res., 19(6) (2004) 1849-54
7. M. D. Maeder, D. Damjanovic, N. Setter, J. Electroceram., 13, (2004)385-392
8. Y. Li, K. Moon and C. P. Wong, Science., 308(2005) 1419-1420
9. T. Maiti, R. Guo, and A. S. Bhalla, J. Appl. Phys., 100(11) (2006) 114109-1–6.
10. M.H. Frey, D.A. Payne, "Grain-size effect on structure and phase transformations for barium titanate", Phys. Rev. B, 54 (1996) 3158–3168.
11. M. Yashima, T. Hoshina, D. Ishimura, S. Kobayashi,W. Nakamura, T. Tsurumi, S. Wada, "Grain-size effecton structure and phase transformations for barium titanate",J. Appl. Phys., 98 (2005) 014313.
12. T. Yamamoto, K. Urabe, H. Banno, "BaTiO3 particlesize dependence of ferroelectricity in BaTiO3 /polymer composites", Jpn. J. Appl. Phys., 32 (1993) 4272–4276.
13. B.J. Chu, D.R. Chen, G.R. Li, Q.R. Yin, "Electrical properties of Na1/2Bi1/2TiO3-BaTiO3 ceramics", J. Eur. Ceram. Soc., 22 (2002) 2115–2121.
14. D. Rout, K.S. Moon, V.S. Rao, S.J.L. Kang, "Study of the morphotropic phase boundary in the lead-free Na1/2Bi1/2TiO3-BaTiO3 system by Raman spectroscopy", J. Ceram. Soc. Jpn., 117 [7] (2009) 797–800.
15. K. Pengpat, S. Hanphimol, S. Eitssayeam, U. Intatha, G. Rujijanagul, T. Tunkasiri, "Morphotropic phase boundary and electrical properties of lead-free bismuth sodium lanthanum titanate-barium titanate ceramics", J. Electroceram., 16 (2006) 301–305.
16. W. Jo, J.E. Daniels, J.L. Jones, X. Tan, P.A. Thomas, D. Damjanovic, J. Rödel, "Evolving morphotropic phase boundary in lead-free Bi1/2Na1/2TiO3-BaTiO3 piezoceramics", J. Appl. Phys., 109 (2011) 014110.
17. I.G. Siny, E. Husson, J.M. Beny, S.G. Lushnikov, E.A. Rogacheva, P.P. Syrnikov, "Raman scattering in the relaxor-type ferroelectric Na1/2Bi1/2TiO3", Ferroelectrics, 248 (2000) 57–78.
18. S. Trujillo, J. Kreisel, Q. Jiang, J.H. Smith, A.P. Thomas, P. Bouvier, F. Weiss, "The high-pressure behaviour of Ba-doped
19. Na1/2Bi1/2TiO3 investigated by Raman spectroscopy", J. Phys: Condens. Matter, 17 (2005) 6587–6597.
20. J. Wang, Z. Zhou, J. Xue, "Phase transition, ferroelectric behaviors and domain structures of (Na1/2Bi1/2)1−xTiPbxO3 thin films", Acta Materials, 54 (2006) 1691–1698.
21. D.L. Corker, A.M. Glazer, R.W. Whatmore, A. Stallard, F. Rauth, "A neutron diffraction investigation into rhombohedral phases of the perovskite series PbZr1-xTixO3", J. Phys: Condens. Matter, 10 (1998) 6251–6269.
22. M.S. Zhang, J.F. Scott, "Raman spectroscopy of (Na0.5Bi0.5)TiO3", Ferroelectr. Lett., 6 (1986) 147–152.
23. A.S. Barker, A.J. Sievers, "Optical studies of the vibrational properties of disordered solids", Rev. Mod. Phys., 47 (1975) S1–S179 Suppl No 2, 180.
24. J. Kreisel, B. Dkhil, P. Bouvier, J.M. Kiat, "Effect of high pressure on relaxor ferroelectrics", Phys. Rev., B, 65 (2002) 172101-1
25. H. Uwe, K.B. Lyons, H.L. Carter, P.A. Fleury, "Ferroelectric micro regions and Raman scattering in KTaO3", Phys. Rev. B, 33 (1986) 6436–6440.
26. H. Uwe, K.B. Lyons, H.L. Carter, P.A. Fleury, "Ferroelectric micro regions and Raman scattering in KTaO3", Phys. Rev. B, 33 (1986) 6436–6440.
27. Kraus W, Nolze G: POWDER CELL- a program for the representation and manipulation of crystal structures and calculation of the resulting X-ray powder patterns. J Appl Cryst 1996, 29:301-303
28. Aksel E,Forrester JS Foronda HM,Dittmer R,Damjanvic D.Jones JT.JAppl Phys 2012:112:054111.
29. D. A. Tenne, A. Soukiassian, X. Choosuwan, R. Guo, A. S. Bhalla, Phys.Rev. B 2004, 70, 174302.
30. A. M. Mathai, R. S. Katiyar, J. Math. Sci. 1996, 81, 2454.